Spring 2023

Deposited Cigarette Smoke as a Driver of Oxidation and Partitioning Processes on Indoor Surfaces

April Hurlock
Bucknell University, amh049@bucknell.edu

**Deposited Cigarette Smoke as a Driver of Oxidation and
Partitioning Processes on Indoor Surfaces**

by

April M. Hurlock

A Thesis Submitted to the Honors
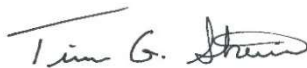Council For Honors in Chemistry

April 7, 2023

Approved by:

Adviser: _____

Douglas B. Collins

Second Evaluator: _____

Timothy G. Strein

Honors Council Representative: _____

Moria C. Chambers

Department Chair: _____

Karen J. Castle

Acknowledgements

I want to start off by thanking Dr. Collins for all of the mentorship and guidance that he has provided me over the last four years, both in and out of the research lab. From the start, I was trusted with a novel, independent research project which has allowed me to grow as a student, researcher, and an individual, so I am incredibly grateful for the invaluable experience I have gained. I would also like to thank the entire Collins lab for the support and community that it has brought me over the past four years. Specifically, I would like to thank Maggie Young, Naomi Douek, and Olivia Jaye for working on related parts of my project, allowing it to grow beyond the scope of this thesis.

I am also incredibly grateful for the Bucknell Chemistry Department. As soon as I stepped onto campus, the entire department – faculty, staff, and students – welcomed me with open arms. I would especially like to thank Dr. S. Smith for being a phenomenal mentor and role model for me during the last four years.

I also want to extend a special thank you to the two additional professors on my Honors Committee, Dr. Strein and Dr. Chambers, for their time, flexibility, and support throughout this entire process.

Finally, I would like to thank my funding sources for this research including the NSF-funded STEM Scholars program, the NSF-funded Physical Sciences Scholarship, the Alfred P. Sloan Foundation, and the NSF Major Instrumentation grant.

Table of Contents

Figures & Tables List

Abstract

Despite the large amount of time that individuals spend indoors during their lives, very little attention was paid to the chemistry that occurs on indoor surfaces until recently. Although not visible to the naked eye, physical and chemical processes, such as partitioning and oxidation, are occurring on virtually every indoor surface in a typical household. Indoor pollutants, ranging from skin oils to environmental cigarette smoke, drive a lot of these processes. The transformation of indoor surfaces by indoor pollutants can increase chemical exposure risks as new irritants or carcinogens can be introduced to the surfaces. In this thesis, I describe a series of studies that used cigarette smoke as a proxy for reactive oxygen species to investigate how surface composition is altered after exposure to an indoor pollutant. Early work on this project focused on designing the smoking apparatus and optimizing experimental methods. After constructing a more controlled system, cigarette smoke was deposited onto glass substrates that were pre-coated with different surface films. The molecules that were present on the surface of the substrate were analyzed at specific time intervals with high-resolution mass spectrometry. Temporal trends of 4 tobacco alkaloids – nicotine, cotinine, N-formylnornicotine, and nicotelline – and nicotine oxide were analyzed over the course of 1 week. The relative changes in these compounds over time were notably different in the presence and absence of a surface film. In the presence of a surface film, the tobacco alkaloids increased, likely in part due to partitioning. Analysis of oleic acid and squalene surface films when exposed to

cigarette smoke revealed the formation of multiple oxidation products, many of which shared the same molecular formula. Ongoing analysis is being conducted to propose the chemical structures of these compounds. Future studies will expand this work to encompass the diversity of indoor environments by investigating different types of surface films, surface materials, and sources of reactive oxygen species.

1. Introduction

People spend about 90% of their lives in indoor environments.[1] During this time, they come in contact with both indoor air and a variety of different indoor surfaces. These surfaces consist of not only the solid material they are made out of but also a wide variety of deposited chemicals, oils, and pollutants from the humans that occupy these spaces as well as other environmental sources such as cooking, smoking, and cleaning. Every dinner prepared, candle lit, and cleaner sprayed introduces a new layer of complexity to the indoor spaces we occupy. While not apparent to the naked eye, many physical and chemical processes occur in indoor air and on every indoor surface, introducing new compounds to the environment, some of which can be harmful to humans and household pets.[2–5] Due to the significant amount of time that people spend indoors, high exposure risks are present for humans and household pets in homes, offices, and other enclosed spaces. Investigating indoor processes will lead to a better understanding of these risks and the development of more informed regulations, building operations, and cleaning procedures.

Indoor environments have distinct properties from outdoor environments such as low levels or a lack of direct sunlight, rain, wind, and strong temperature fluctuations; however, indoor air is constantly mixing and exchanging with outdoor air. Depending on the type of building, it can take anywhere from 28 min to 11 hours to completely exchange the indoor air with outdoor air.[6] This consistent

turnover means that indoor chemical equilibria are frequently disrupted and seek re-establishment as new air and suspended particles are being introduced. Despite exchange with outdoor air, indoor environments have a much higher concentration of volatile organic compounds, ranging from 2-80 times that of outdoor levels for any individual compound.[7] These elevated concentrations, in conjunction with the fact that indoor environments exhibit a much larger surface area-to-volume ratio than outdoor environments, make indoor surfaces a prime location for complex processes involving both the airborne chemicals in the gas phase and deposited chemicals in the condensed phase.[8]

Surface materials in indoor environments are incredibly diverse in chemical composition. Surfaces can be organic (e.g. polyester, nylon, wood, and cotton), inorganic (e.g. glass, concrete, and drywall), or mixed (e.g. latex paint) in nature.[9] These classifications are assigned based on the elements that make up the structures of each of these materials: organic surfaces consist of carbon, hydrogen, oxygen, and nitrogen while inorganic surfaces contain metals or metalloids in addition to the organic nonmetals. The differences in elemental composition of these surfaces translate into differences in properties such as porosity, water absorption, and reactivity. These properties drive different chemical and physical processes on their respective surfaces, contributing to the constantly evolving nature of indoor environments.

An additional layer of complexity arises when the deposition of chemical films on these surfaces is considered.[10] Environmental films can be composed of

deposited particulate matter, skin oils, dust, and chemicals from cleaning products, decorative coatings, pesticides, and even living microbes.[11,12] Films that form on indoor surfaces can strongly control the air quality inside a building and human exposure to environmental contaminants.[13] The chemical composition of both the gas phase and condensed (surface film) phase in indoor environments are in a continuous, dynamic exchange. The process by which chemicals transfer between physical phases is referred to as 'partitioning'. The chemical composition of both the gaseous and condensed phases may be transformed through reactions, although chemistry within indoor surface films has been weakly studied to date.

Surface complexity presents many challenges when studying indoor environments. A variety of chemicals with different properties and abundances are present on most surfaces,[9,12] so analytical techniques used to analyze these systems must be sensitive and have a high resolution. Mass spectrometry (MS) has become a popular choice to study indoor surface chemistry due to its versatility and high resolution.[14] MS allows for the masses of different chemicals in a sample to be determined. Molecules in a sample are ionized and the mass-to-charge (m/z) ratios are measured by a detector. For the vast majority of small molecules, the ion charge (z) is equal to 1, so the m/z value can be thought of as the mass of the ion. High-resolution mass spectrometry (HR-MS) allows for exact masses to be measured to four decimal places rather than just integer masses, which allows for confident assignment of molecular formulas based on m/z alone.[15] In complex media such as surface films, many chemicals in the sample could share the same

nominal mass but have different elemental composition or structure. Some HR-MS instruments are capable of providing information to support molecular structure identification using tandem MS (MS/MS or MS[2]), in which ions of a certain m/z are selected, then fragmented by collision with inert gas molecules.[16] The m/z values of the various fragments can be used to deduce the connectivity or structure of the molecule, even if there are multiple chemicals with the same exact mass. High resolution quadrupole time-of-flight (Q-ToF) MS is well suited to both HR-MS and MS/MS tasks. Overall, HR-MS and MS/MS are powerful tools used to study specific compounds and can prove critical in tracking individual compounds when the system undergoes chemical changes over time.

Chemistry can occur on air-exposed surfaces in a variety of ways. Semi-volatile organic compounds (SVOCs) can partition between the surface and gas phases in both directions, contributing to changes in surface composition without chemical reactions taking place.[17] When reactions occur within the surface film, altering its chemical composition, the exposure risks associated with the surface film may evolve over time. Reactive oxygen species (ROS), produced as a result of multiphase reactions with trace gases, have been shown to initiate oxidation on surfaces by reacting with the chemical surface films.[9] Products of these reactions, such as peroxides and hydroperoxides, can lead to inflammation and other adverse health effects.[2–5] Studying such reactions in indoor environments can reveal potentially harmful oxidative chemical pathways that are occurring on household surfaces.

It is well known that cigarette smoke particles contain significant amounts of ROS.[18] Cigarette smoke that deposits on indoor surfaces, known as third-hand smoke (THS), represents a long-term reservoir of toxic chemicals in an indoor environment.[19] Cigarette smoke particles can deposit on surfaces from direct exposure to smoking but also from being taken up by ventilation systems and brought indoors,[20] so exposure may occur even if smoking-designated areas are located directly outside buildings. THS-containing chemical films can persist on household surfaces and initiate reactions with other chemicals found in the environment, producing harmful byproducts such as carcinogenic tobacco-specific nitrosamines.[21,22] Chemicals and byproducts found in surface films, including those associated with THS, can be introduced into the body through skin contact with contaminated surfaces as well as ingestion and inhalation.[23] Preliminary experiments have shown that THS has the ability to damage genetic information in humans and can cause complications such as metabolic syndrome, fibrosis, poor wound healing, and hyperactivity in mouse models.[24,25]

A variety of studies have investigated the composition, reactivity, and toxicity of gaseous tobacco-related chemicals in indoor environments, in concert with other indoor pollutants.[26–29] For example, THS has been shown to react with ozone[26,27,29] and nitrous acid,[22] two prominent indoor gas-phase pollutants, to produce harmful byproducts. However, far less is currently known about the potential for chemistry to occur within THS films without the influence of reactive trace gases, the influence of THS films on the composition and chemical processes

that occur on air-exposed indoor surfaces, and the environmental factors that may influence the indoor multiphase chemistry of THS. As previously discussed, due to the high exposure risks associated with indoor surfaces as well as the health risks associated with THS, research is needed to understand condensed-phase reactions associated with THS deposition.

In this thesis, I have investigated the complex relationship between deposited cigarette smoke residue and the surface on which it is deposited in order to probe the effects of ROS and SVOCs on indoor surface chemistry. By considering the oxidation driven by deposited particles in addition to the well-characterized partitioning processes, a more accurate picture of indoor surface chemistry can be obtained (Figure 1). Cigarette smoke is also being used as a model system for other particulate matter sources that exist indoors that may have oxidative behavior, like wood smoke, cooking emissions, or traffic-related air pollutants that are transported in from outdoors.[30,31] My findings show that cigarette smoke deposition leads to oxidation of some components that are present in typical indoor surface films and that the presence of a pre-existing surface film influences the abundances of semi-volatile THS components over a one-week timescale.
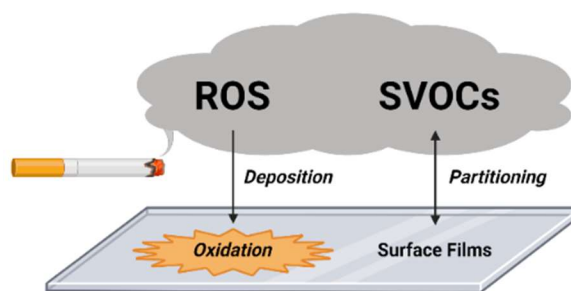
Figure 1. A schematic of the chemical and physical processes of cigarette smoke in indoor environments. Reactive oxygen species (ROS) can deposit onto surfaces and participate in oxidation reactions while semi-volatile organic compounds (SVOCs) can partition between the gas and condensed phases.

2. Study Design

Early stages of this project in 2019 were exploratory in nature. With very little existing research on the condensed phase of THS in the published literature at that time, the first few months of this research were dedicated to crude, untargeted chemical analyses to develop an informed and testable hypothesis. Preliminary experiments attempted to maximize the amount of smoke collected in order to facilitate qualitative analysis of THS films. To achieve this, cigarettes were smoked directly into 20-mL glass scintillation vials until visibly saturated with smoke. Then, the vials were sealed and let sit until the gas inside the vial was transparent, indicating that the particulate matter had deposited on the glass inside the vial. The deposited smoke was then extracted in HPLC-grade methanol. To fully extract the deposited particles, the vials were placed on their side on the Nostalgia Countertop Hot Dog Roller without heat for 5 min. The extracted compounds were analyzed using flow injection analysis with high-resolution Orbitrap mass spectrometry (Exactive, Thermo Scientific).

My first experiments revealed the dynamic nature of deposited cigarette smoke. An untargeted analysis indicated that the abundance of some compounds increased over time while others decreased over time within the deposited cigarette smoke film within a sealed container. These temporal trends did not necessarily indicate reactivity, however, because changes in the abundance of semi-volatile organic compounds in the literature had been ascribed to

partitioning.[17] Instead, it was one trend in particular, the formation of nicotine oxide, which alluded to the presence of oxidation pathways in cigarette smoke residue. This discovery shaped the project, resulting in its first major investigative question: how does the presence of a surface film impact the oxidative chemistry associated with deposited cigarette smoke? I formulated a plan to test various antioxidants and surface films to understand the complex relationship between these chemicals. Over time, the project evolved to focus more on the surface film than the smoke residue. While the early experiments were critical in developing hypotheses and the future of the project, the crude methodology lacked important controls and quantitative replicability. Therefore, before reliable data could be collected, apparatus and method development were necessary.

The first major objective to standardize these experiments was to design and assemble an apparatus for controlled smoke deposition (Figure 2). The first prototype of the smoking apparatus consisted of a side-arm flask, faucet aspirator, and aquarium pump connected with Tygon tubing (Figure 2B). The cigarette was fastened into a fitting that was under suction from an aspirator. Puffing was simulated by squeezing the tubing between the cigarette and the aspirator. The other end of the cigarette was held inside the side-arm flask to filter the ash and tar from the smoke. Air pumped from the aquarium pump was used to flush the smoke through the side arm of the flask and into a 20-mL scintillation vial for collection.
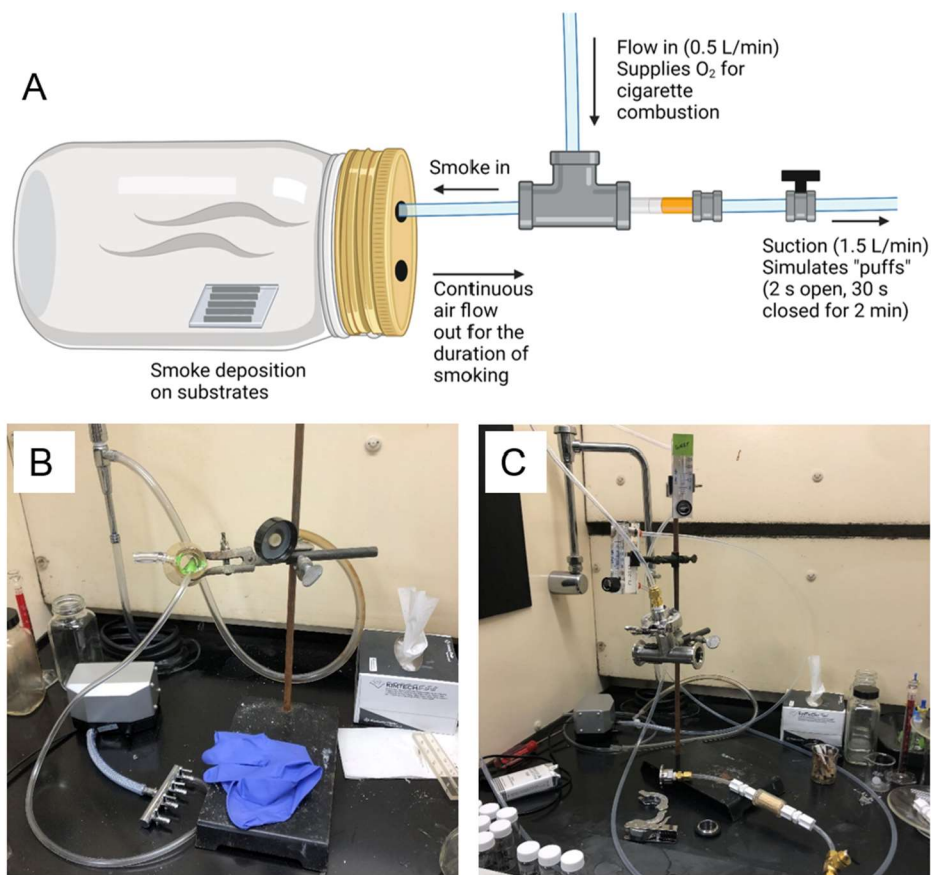
Figure 2. Smoking apparatus set-up. A schematic of the flow of air and cigarette smoke during deposition (A). Images of the set-up before (B) and after (C) apparatus development.

While this crude apparatus was effective in collecting large amounts of smoke to investigate the composition of deposited cigarette smoke in preliminary studies, there were many flaws in the system that would prevent the collection of replicable quantitative results. Primarily, the side-arm flask was not well-sealed and much of the cigarette smoke was released into the surrounding fume hood, so the amount of smoke deposited was not constant across experiments. Secondarily, the simulation of puffing was subject to inconsistencies because it required the experimenter to manually squeeze the tubing by hand. This flaw

further exacerbated inconsistencies in smoke deposition because the force used between "puffs" was not tightly controlled. Finally, this first set-up required two experimenters to operate the apparatus, which made smoke deposition very inconvenient for this independent study.

The current smoking apparatus addresses the flaws of the original set-up. The first major change was to ensure that the system was well-sealed so that the smoke was depositing on the substrate of interest consistently. This was achieved by replacing the side-arm flask with an aluminum KF25 tee connector, brass compression fittings, and PFA tubing (Figure 2C). To control the simulated puffs, a valve was placed in between the cigarette and the suction line. This replaced the manual puff, modifying the experiment so that each puff was exactly the same. Additionally, variable area flow meters with needle valves (Omega Engineering) were placed on both the suction and flow-in lines to set the flow rates and ensure consistency between experiments. Finally, to accompany this controlled apparatus, a standardized smoking procedure, defined by the International Organization for Standardization (ISO), was adopted to increase replicability between experiments and across experimenters.

With the more tightly-controlled apparatus, further decisions needed to be made about the scope of the project. While smoking directly into scintillation vials was convenient for extraction, it was difficult to ensure that the amount of smoke deposited was consistent over multiple vials. Additionally, future studies investigating surface films and non-glass surfaces could not be easily modeled

directly in scintillation vials. Therefore, a smoking chamber was assembled with a 64-oz clear Ball mason jar and glass slide(s) to hold the substrates of interest. Early iterations of this set-up used an amber glass jar, but due to the light-dependent nature of oxidation reactions, we chose to use a clear glass jar with constant illumination from fluorescent lighting to better control the artificial light of indoor environments and maintain experimental consistency.

To investigate the temporal trends of the chemical composition of THS-exposed surfaces, multiple substrates would need to be placed in the smoking chamber and exposed to a consistent amount of smoke. Two different substrate placements were tested: perpendicular to the smoke stream and parallel to the smoke stream. After testing the smoke deposition for each placement, it was determined that the perpendicular placement (shown in Figure 2a) had much more consistent deposition than the parallel placement. This is critical for ensuring that each substrate is starting with the same amount of smoke and that any differences in the composition are due to aging and not inconsistent deposition. In addition to the perpendicular placement, the substrates were mounted in the chamber horizontally, as opposed to upright, to maximize particle deposition.

3. Materials & Methods

3.1. General Experimental Set-up

One major goal of this project was to understand the temporal trends of the cigarette smoke components, the surface films on which the smoke was deposited, and the oxidized byproducts of reactions between the cigarette smoke and the surface films. To investigate how the composition of the THS-exposed surface changes over time, quantitative experiments were conducted in which chemicals on THS-coated substrates at 6 time points were measured over the span of 1 week (0, 24, 48, 72, 96, and 168 h) and focused on relative quantitation of surface chemicals. Another important goal was to identify surface-film oxidation products; however, these compounds were often found in small abundance relative to the cigarette smoke components. To increase signal-to-noise ratio for the oxidation products, qualitative experiments were conducted in which several sample substrates were pooled to concentrate samples so that a greater focus could be placed on finding and identifying new features in the data.

Conducting these different experiments requires different set-ups for the smoking chambers. For timeline experiments, the chambers are prepared with either 6 or 12 substrates, depending on the surface film of choice. Because of the differing solubilities of the different surface films, some experiments require separate extractions for THS components and surface film chemicals. The THS

chemicals of interest are soluble in water, so if the film is similarly soluble in water, 6 substrates were used in the smoking chamber and a single aqueous extraction of the film was used for all target analytes. If the film is weakly soluble in water, then 12 substrates were used: 6 to be extracted in polar solvent to analyze the THS components and 6 to be extracted in nonpolar solvent to analyze the surface film. The substrates for surface film analysis were placed in the chamber directly behind the substrates for THS analysis such that equal deposition of cigarette smoke is still observed.

For the qualitative experiments, the chambers were prepared with 10 substrates, arranged similarly to the timeline experiments that have dissimilar solubilities. However, 5 substrates will be extracted at once for each the 0-h and 168-h samples. This allows for a 5-fold more concentrated sample to identify potential surface film oxidation products.

3.2. Substrates and Substrate Coating

Borosilicate glass substrates were prepared by cutting microscope slides into 1.0 x 2.6 cm rectangles. This size was chosen so that 6 substrates could be placed across the chamber stage to correspond with a 1-week timeline (0, 24, 48, 72, 96, and 168 h). Cut substrates were sonicated in methanol for 30 min to remove any contaminants. After sonication, the solvent was poured off and any remaining methanol was evaporated under N_2 gas.

In order to understand the reactivity of deposited smoke, films of specific chemicals were deposited onto glass substrates before exposing them to cigarette smoke. A non-volatile antioxidant, tris(2-carboxyethyl)phosphine (TCEP), was used to probe the overall oxidative potential of reactive oxygen species in THS. Additionally, bisphenol-A (BPA), a surface contaminant, oleic acid (OA), a prominent cooking oil component, and squalene (SQ), a human skin oil component, were used as proxies for indoor surface films to investigate THS chemistry. Oleic acid did not deposit in an even film on glass, so it was first combined with bis(2-ethylhexyl) sebacate (BES), a non-reactive oil. Solutions of each of these surface coatings were made at a concentration of 9 mM, each chemical in a solvent that would completely dissolve the coating and evaporate readily to enable surface film deposition (Table 1). To deposit the coating, 25.0 µL of the respective solution (225 µmol of each surface chemical) was spread evenly over the top side of the glass substrate and the solvent was evaporated under N_2 gas.

Table 1. Solvents for each of the surface coating stock solutions. Each solution was made to a concentration of approximately 9 mM.

Surface Coating	Solvent
TCEP	Methanol (MeOH)
BPA	MeOH
OA	Acetonitrile (ACN)
BES	Isopropanol (IPA)
SQ	ACN

To probe reactions on non-glass surfaces, cellulose filter paper was used as the substrate. Glass is a relatively nonreactive, non-porous substrate, so to better characterize the diverse surface compositions found in indoor environments, porous materials need to be explored. Indoor environments are commonly occupied by wood and cotton surfaces, materials that can be modelled with cellulose, a related organic polymer. Cellulose substrates (Fisherbrand Qualitative Grade Plain Filter Paper Circles - P5 Grade) were cut to 1.0 x 2.6 cm rectangles. After being cut, the substrates were placed in the chamber for smoke deposition.

3.3. Smoke Generation and Deposition

Smoke generation was carried out following the ISO standardized protocol using 1R6F research cigarettes (University of Kentucky).[32] After the cigarette was lit and placed into the smoking apparatus, puffs were simulated for 2 s every 30 s for 2 min. The smoking chamber was then sealed and the smoke was allowed to deposit to surfaces within the chamber for 30 min. After deposition, 0-h samples were promptly removed from the chamber for analysis. Based on the time scale of each experiment, subsequent substrates were removed at designated intervals.

3.4. Liquid Extraction

For each time point in the quantitative experiments, a single substrate was extracted (or two substrates if separate extractions were needed for the THS components and the surface film). Substrates were removed from the smoking chamber and placed into 20-mL scintillation vials. The appropriate extraction solvents and internal standard (IS) were added to the vials (Table 2). An ammonium formate buffer (90% aqueous 10 mM NH_4HCO_2, 10% MeOH, pH 8.5) was used for the polar extraction solvent, which matched the aqueous component of the mobile phase gradient (see also Section 3.5). An acetaminophen solution (stock concentration: 0.42 mg/mL) was used as the internal standard to control for instrument variation between samples. To ensure the entire substrate is sampled evenly, the vials are placed on their side on a standard analog rocker (VWR) for 10 minutes on each side. After extraction is complete, the solutions were transferred to amber glass 2.0-mL autosampler vials (Agilent Technologies) for liquid chromatography mass spectrometry (LC-MS) analysis.

To ensure that qualitative extractions were as concentrated as possible, substrates were extracted sequentially in the same aliquot of extraction solvent to maximize film extraction and minimize solvent used. First, two substrates were extracted in 2.0 mL of the appropriate extraction solvent. Since this analysis was focused on surface-film oxidation products, only the surface film extraction solvents were used. The first two substrates were placed on the rocking table, 10

minutes on each side, to fully extract. Then, the first two substrates were removed, ensuring that no solvent is lost, and replaced with the final three substrates. These substrates were extracted in the same solvent, 10 minutes on each side. After all substrates were extracted for the appropriate sample, the solution was transferred to an amber glass 2.0-mL autosampler vial (Agilent Technologies) for LC-MS analysis.

Table 2. Extraction methods for each surface film. The volumes presented were used for quantitative studies. For qualitative studies, the volumes for the solvents were doubled. The internal standard used was acetaminophen (0.42 mg/mL stock concentration).

Film Material	Surface Film Extraction
[none] TCEP BPA BES	0.900 mL ammonium formate buffer, 0.100 mL IS
OA/BES SQ	0.450 mL dH$_2$O, 0.450 mL ACN, 0.100 mL IS

3.5. Instrumental Analysis

For each time point analyzed, samples and blanks were prepared and run in triplicate. A solvent blank, which contained just the extraction solvent, and an extraction blank, which was prepared by extracting a clean substrate, were run with every set of samples. A negative control, a substrate coated with a surface film that was not exposed to THS, would be extracted and analyzed alongside the 0-h samples to account for any reactivity that would occur during the deposition and extraction processes.

Reverse-phase liquid chromatography (LC) was used to separate detected compounds. A Kinetex EVO C18 LC column (5 μm, 100 x 3.0 mm; Phenomenex, Inc.) was selected for the chromatography. LC methods were developed based on the compounds they were meant to separate. The mobile phase compositions and gradients were chosen with the goal of maximizing the resolution for the compounds of interest while minimizing run time (Table 3).

Table 3. LC-MS methods to separate the compounds of interest for each type of analyte. The mobile phases used were water (0.1% formic acid) (A), acetonitrile (B), ammonium formate buffer (90% aqueous 10 mM NH_4HCO_2, 10% MeOH, pH 8.5) (C), and MeOH (D). All methods used a flow rate of 0.400 mL/min.

Analyte	Chromatographic Method
Tobacco Alkaloids TCEP BPA	10% D and 90% C for 1 min, 10-95% D for 4 min, hold 95% D for 5 min, 5-90% C for 0.25 min; 3 min equilibration time
OA	5% A and 95% B for 5 min
SQ	50% A and 50% B for 1 min, 50-100% B for 2 min, hold 100% B for 13 min, 0-50% A for 0.1 min; 4 min equilibration time

Early experiments in this project used high-resolution Orbitrap mass spectrometry to analyze extracted samples, but the majority of the experiments used Quadrupole Time-of-Flight (Q-ToF) mass spectrometry, which granted automation and tandem MS capabilities. All experiments were run in electrospray ionization mode (ESI) with the exception of squalene analysis which was run in atmospheric-pressure chemical ionization mode (APCI). APCI has a better ionization efficiency for nonpolar compounds such as squalene. The Orbitrap mass spectrometer (Exactive, ThermoFisher Scientific) was fitted with an Ion Max

heated electrospray ionization (HESI) ion source and liquid handling was performed with an Accela 1260 quaternary pump. The sample loop had a fixed volume of 10 µL. The Orbitrap system did not have thermal control for liquid chromatography columns, so all separations were done at room temperature (20-22 °C). The Q-ToF MS (Model 6560, Agilent Technologies) is capable of ion mobility separations but in this study was used in "Q-ToF only" mode. It was fitted with an Agilent Jet Stream ion source for all ESI experiments and a standard APCI source for squalene experiments. An Agilent 1290 Infinity ultra-high performance liquid chromatograph with a quaternary pump, automated multi-sampler, and temperature-controlled column compartment (held at 20 °C) operated ahead of the Q-ToF MS. Injection volume was 2.00 µL. Parameters for each mass spectrometry method are displayed in Table 4.

Table 4. Parameters for Q-ToF mass spectrometry experiments.

ESI Mode

Method ID	A	B
Analyte(s)	Tobacco Alkaloids, TCEP, BPA	OA
Acquisition Range (m/z)	50-1700	50-1700
Acquisition Rate (spectra/s)	10	10
Polarity	+	-
Gas Temp (°C)	325	325
Drying Gas (L/min)	13	13
Nebulizer (psi)	35	20
Sheath Gas Temp (°C)	275	300
Sheath Gas Flow (L/min)	11	10
Capillary Voltage (V)	4000	4000
Nozzle Voltage (V)	0	0
Fragmentor Voltage (V)	400	400

APCI Mode

Method	C
Analyte(s)	SQ
Acquisition Range (m/z)	50-1700
Acquisition Rate (spectra/s)	5
Polarity	+
Gas Temp (°C)	325
Vaporizer (°C)	500
Drying Gas (L/min)	8
Nebulizer (psi)	35
Capillary Voltage (V)	1900
Corona+ (μA)	4
Fragmentor Voltage (V)	400

Tandem mass spectrometry (MS/MS) was used to confirm the identities of the tobacco alkaloids and oxidation products. The previously-described MS Methods A and C were modified to include settings for targeted MS/MS analysis (Table 5). Fatty acids, such as oleic acid, are not susceptible to fragmentation, so Method B was run in HR-MS mode only.

Table 5. MS/MS target lists for fragmentation.

Method A

Analyte(s)	Tobacco Alkaloids	
Acquisition Range (m/z)	50-1700	
Acquisition Rate (spectra/s)	5	

Target List

Precursor Mass (m/z)	Iso Width	Collision Energy (eV)
152.0706	Narrow (~1.3 m/z)	20
163.1230	Narrow (~1.3 m/z)	20
177.1026	Narrow (~1.3 m/z)	20
179.1181	Narrow (~1.3 m/z)	20
234.1031	Narrow (~1.3 m/z)	30

Method C

Analyte(s)	SQ oxidation products	
Acquisition Range (m/z)	30-1700	
Acquisition Rate (spectra/s)	3	

Target List

Precursor Mass (m/z)	Iso Width	Collision Energy (eV)
425.3766	Narrow (~1.3 m/z)	20
427.3928	Narrow (~1.3 m/z)	15

3.6. Data Analysis

Quantitative analysis was carried out using Skyline (MacCoss Lab Software), from which the average and standard deviations for normalized peak areas were obtained. The mean peak areas were divided by the mean peak area of the 0-h sample and plotted in Igor Pro 9. Qualitative analysis was carried out using Agilent MassHunter Qualitative Analysis 10.0.

4. Results & Discussion

4.1. THS Suspect Screening

The composition of aged cigarette smoke on clean glass was analyzed with an untargeted LC-MS approach. The mass-to-charge ratios detected were compared with a list of known compounds in cigarette smoke[33] and any matches that had an absolute peak height above 10^4 counts were selected for further analysis. Based on this criterion, ten mass-to-charge ratios were selected. The selected mass-to-charge ratios, retention times (RTs), and putative matches are listed in Table 6. Eight out of the ten mass-to-charge ratios had a single chromatographic peak, while m/z 177 and m/z 179 had two chromatographic peaks (Figure 3b and 3c), indicating that two isomers (same elemental composition, different structure) were separated. Further analysis was needed to identify these isomers.

Table 6. Selected m/z values and associated information for tobacco-related compounds in THS samples.

Measured m/z [M+H]⁺	RT (min)	Label	Putative Match(es)	Predicted Formula	Predicted m/z [M+H]⁺	m/z diff (ppm)
147.0922	5.44	mz147	Myosmine	C9H10N2	147.0922	0.0
149.1079	4.14	mz149	Nornicotine	C9H12N2	149.1073	4.0
157.0766	5.76	mz157	2,3'-bipyridine	C10H8N2	157.0760	3.8
161.1079	6.22	mz161	N-methylmyosmine, anabaseine, anatabine	C10H12N2	161.1073	3.7
163.1231	5.95	mz163	Nicotine	C10H14N2	163.1230	0.6
177.1026	4.15 / 4.37	mz177a / mz177b	Cotinine / N-formylnornicotine	C10H12N2O2	177.1022	2.3
179.1181	1.96 / 2.10	mz179a / mz179b	Nicotine 1'-N-oxides	C10H14N2O	179.1179	1.1
193.0501	4.41	mz193	Scopoletin	C10H8O4	193.0495	3.1
234.1031	6.30	mz234	Nicotelline	C15H11N3	234.1026	2.1
240.1501	6.90	mz240	Anatalline	C15H17N3	240.1495	2.5

To identify notable trends among the selected compounds, a relative quantitation approach was utilized. For each sample extracted at a single time point (t), the peak area (A) for each compound (j) was first normalized to the peak area of the internal standard (IS) for each repeated measurement (i). The

normalized areas were then averaged over the total number of repeated trials (n) to obtain an average normalized signal ($\bar{S}_{norm}$; Eq. 1). Three repeat measurements were obtained from all time points in all experiments.

$$\bar{S}_{norm} = \frac{1}{n}\sum_{i=1}^{n}\left(\frac{A_{i,j,t}}{IS_{i,t}}\right) \qquad\qquad (\text{Eq. 1})$$

For comparisons within each experiment, the value of $\bar{S}_{norm,j,t}$ for each compound at each time point was divided by $\bar{S}_{norm,j,t=0}$ for the 0-h sample, which was collected just after smoke finished setting on the glass substrates. Based on the temporal trends of $\bar{S}_{norm}$, the compounds in Table 6 were placed in three broad categories: increasing, decreasing, and remaining constant over the course of a week (Figure 3a). Two compounds, labelled mz179a and mz179b, exhibited an 80-fold and 22-fold increase, respectively, over the course of a week. Six compounds were observed to have decreased over the course of a week: mz147, mz157, mz161, mz163, mz193, and mz240. These compounds decreased to values 0.7% to 50% of their original concentrations. Four compounds, mz149, mz177a, mz177b, and mz234, exhibited no significant change over the course of the week. Further analysis using tandem mass spectrometry was needed to identify the compounds separated.
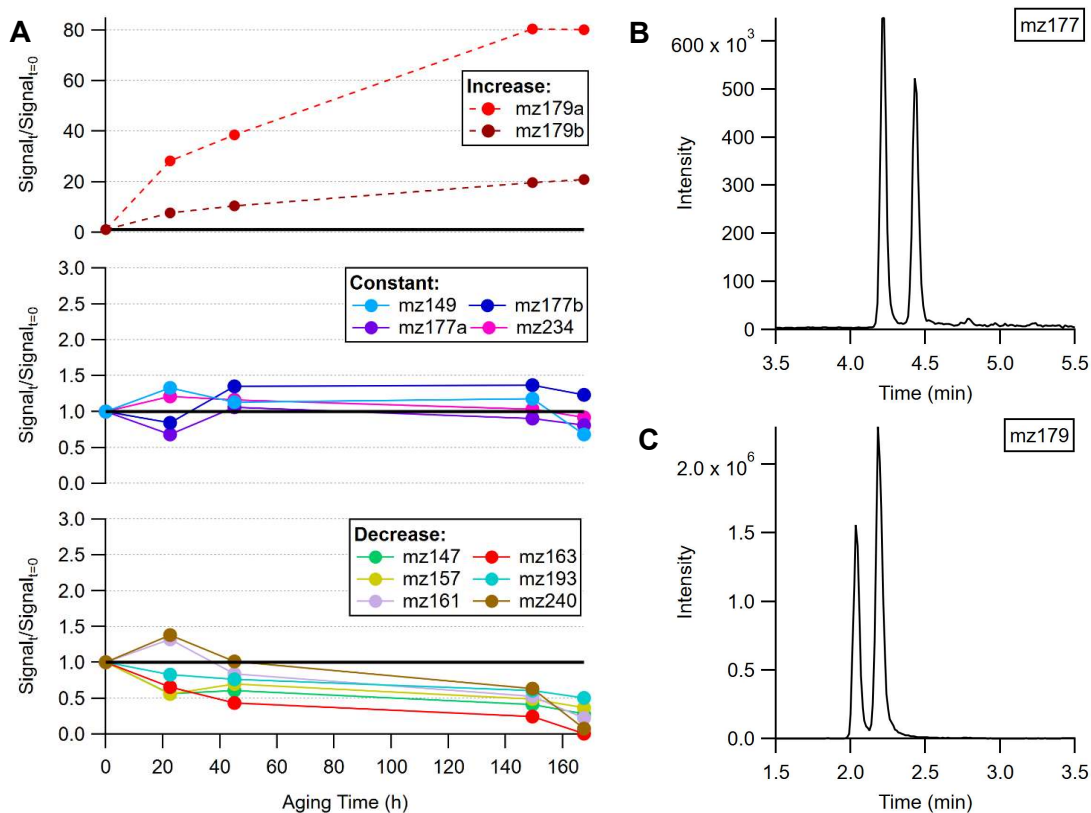
Figure 3. Qualitative suspect screening of deposited cigarette smoke. (A) Relative quantitative trends of selected THS compounds, grouped by their temporal trend (increase, decrease, or remain the same over time). (B) Extracted ion chromatogram for m/z 177.1026. (C) Extracted ion chromatogram for m/z 179.1181. EICs are extracted with a range of ±0.15 m/z relative to the exact mass.

4.2. Identification of Tobacco Alkaloids by MS/MS Analysis

Four tobacco alkaloids – nicotine, cotinine, N-formylnornicotine, and nicotelline – were chosen for further analysis based on their prevalence in THS samples and prior characterization in the literature (Figure 4). Nicotine is a prominent alkaloid in cigarette smoke that can be readily oxidized to form minor tobacco alkaloids and other oxidation products.[34] Cotinine is known to be a major

metabolite of nicotine in biological systems and is a useful biomarker of cigarette smoke exposure due to its prolonged half-life; it has also been implicated as a multiphase oxidation product of nicotine.[35] N-formylnornicotine is a constitutional isomer of cotinine and a lesser-studied minor tobacco alkaloid.[36] Nicotelline, an unreactive tricyclic alkaloid, has been proposed to be a preferential tracer for tobacco smoke and THS.[37]
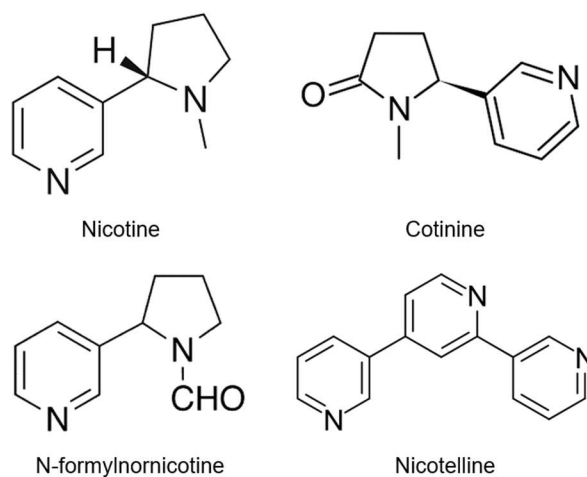

Figure 4. Structures of the tobacco alkaloids chosen for quantitative analysis.

The selected compounds were analyzed using LC-MS/MS to fragment and confirm the identities of these compounds (Figure 5). The fragmentation pattern of a molecule is characteristic of its chemical structure, so it acts like a chemical fingerprint, unique to every molecule with the same chemical connectivity. The experimental fragmentation data was compared to published MS^2 spectra for each of the alkaloids. Nicotine was confirmed as the mz163 compound, validated by m/z fragments 132, 130, 117, 106, 84, and 80.[38] The prediction of nicotelline as mz234 was further supported by the presence of m/z fragments 207 and 155.[37] Nicotelline

had poor fragmentation at a collision energy (CE) of 20 eV (i.e. the CE used for the other tobacco alkaloids), so the CE was incrementally increased to optimize fragmentation. A collision energy of 30 eV was sufficient to confirm the presence of fragments 207 and 155.

Exact mass data can be related to a molecular formula, but organic molecules of identical elemental composition can adopt multiple structures. For the two exact masses that indicated chromatographically separable isomers, MS/MS was used to determine their identities. There are two main classes of isomers: constitutional isomers and stereoisomers. Constitutional isomers have the same chemical formula but different atom connectivity within the molecules. Stereoisomers have the same chemical formula and the same atom connectivity but differ in the orientation of the atoms in space. Constitutional isomers will have different MS^2 spectra because different atom connectivity will result in different fragments, while stereoisomers will have the same MS^2 spectra because they have the same connectivity.

For the isomers with m/z 177.1026, the MS/MS spectra of the two chromatographic peaks were notably different, so it can be concluded that these isomers were constitutional. By comparing MS^2 spectra collected in each chromatographic peak with the literature, it was determined that cotinine eluted first, followed by N-formylnornicotine. The characteristic fragments for each spectra are m/z 98 and 80 for cotinine and m/z 159 and 132 for N-formylnornicotine.[39]
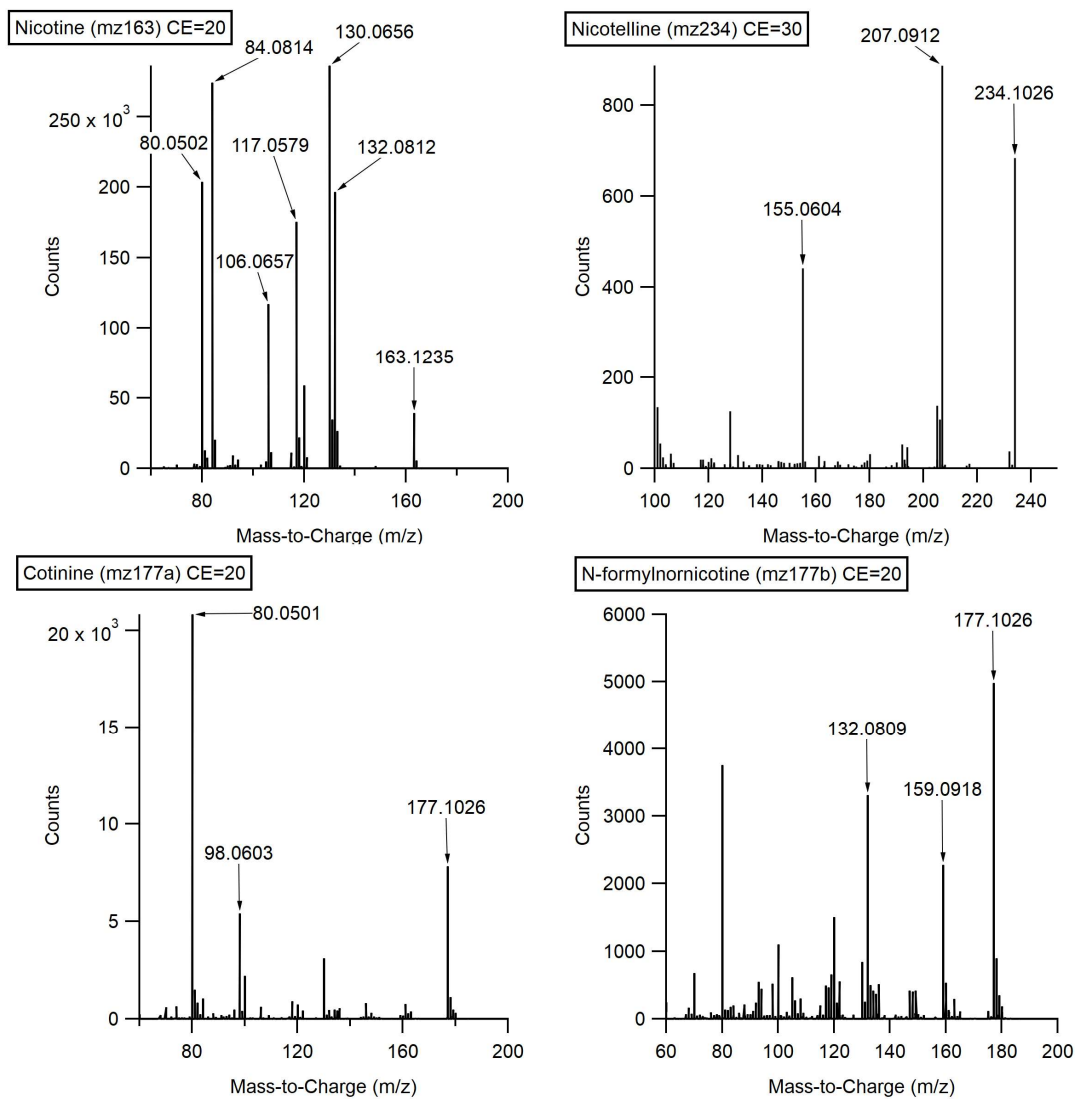
Figure 5. MS/MS spectra for the four prominent tobacco alkaloids: nicotine, cotinine, N-formylnornicotine, and nicotelline. Characteristic fragment peaks are labeled with the exact mass-to-charge ratios.

4.3. Nicotine Oxide Isomer Determination

To determine which two nicotine oxide isomers were separated, LC-MS/MS was used to fragment the compounds with a nominal mass-to-charge ratio of 179. The experimental fragmentation data was compared to published MS^2 spectra for the three possible nicotine oxide isomers (Figure 6a).[40] There is a single stereoisomer for nicotine-1-*N*-oxide and two stereoisomers for nicotine-1'-*N*-oxide. Prominent fragments for nicotine-1-*N*-oxide include m/z 148, m/z 131, and m/z 130 while prominent fragments for nicotine-1'-*N*-oxide include m/z 132 and m/z 130. The difference in fragmentation is the result of which nitrogen on nicotine gets oxidized. Since the two experimental MS/MS spectra are almost identical, and m/z 132 is detected, it can be concluded that the compounds are nicotine 1'-*N*-oxide diastereomers rather than constitutional isomers (Figure 6b).
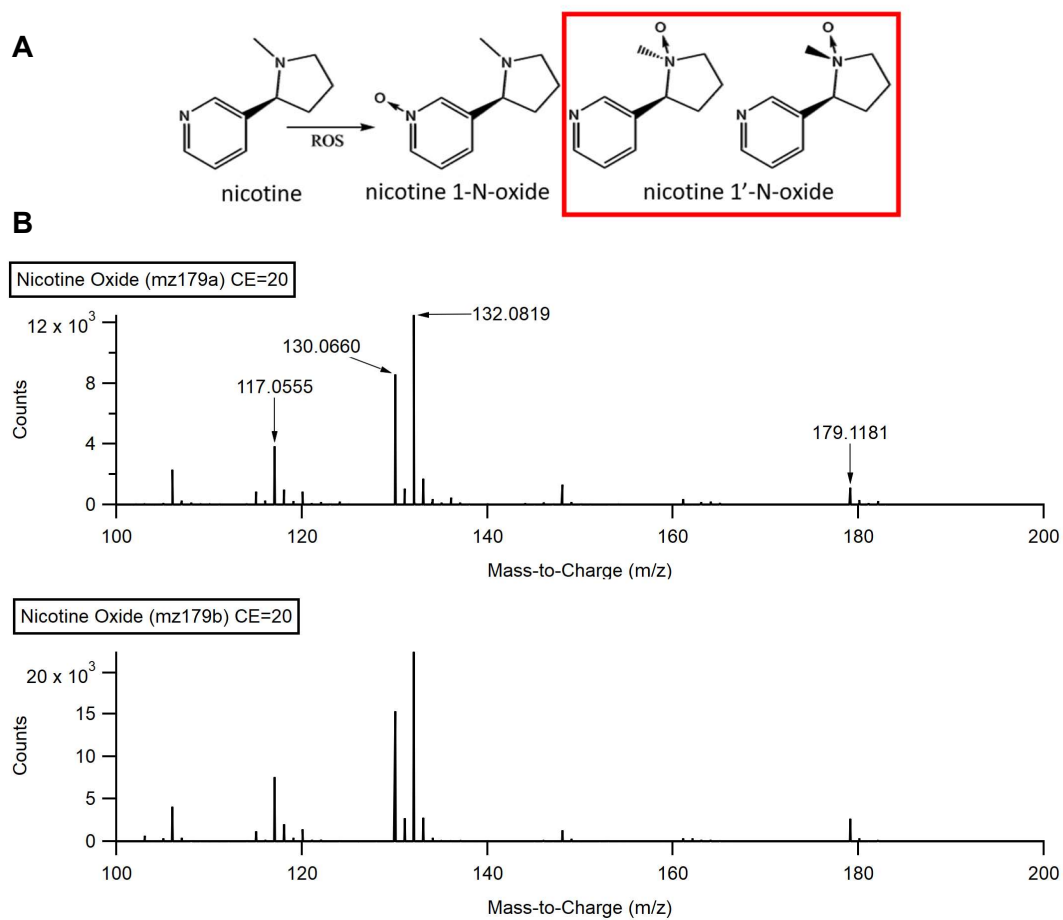
Figure 6. MS/MS analysis of nicotine oxide isomers. (A) Oxidation of nicotine into its possible nicotine oxide isomers. The red box indicates the diastereomers that were identified by MS^2 analysis. (B) MS/MS spectra of mz179a and mz179b. The similar spectra indicate the presence of stereoisomers.

4.4. Targeted Analysis on Clean Glass

The identified alkaloids and nicotine oxides were used to quantitatively study the temporal trends associated with THS (Figure 7). As stated previously, the high abundances of these compounds and their preliminary temporal trends made these alkaloids good targets to study. Nicotine and nicotine oxide were used to probe the oxidative pathways occurring within the smoke, cotinine and N-formylnornicotine, two compounds believed to be fairly unreactive based on preliminary studies, were used to probe partitioning processes that were occurring, and nicotelline, an unreactive and low-volatility compound, was used to ensure consistent deposition and extraction over the course of the experiments.
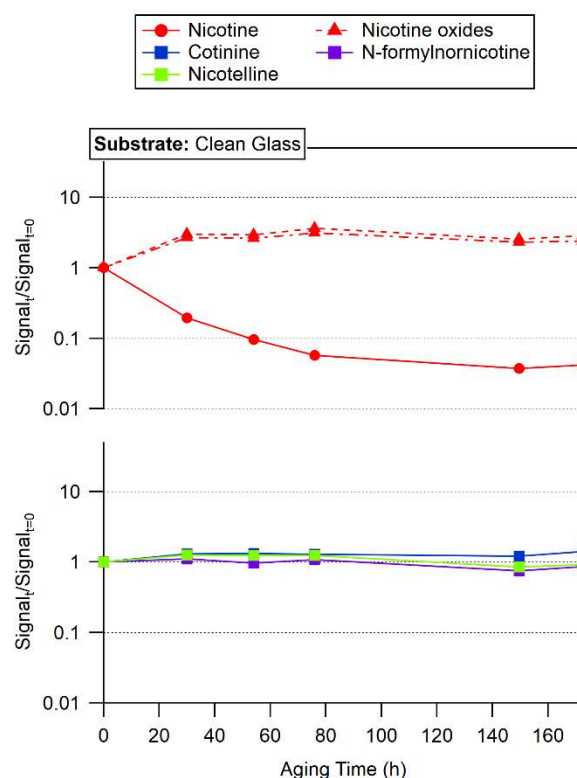

Figure 7. Temporal trends of tobacco alkaloids on clean glass relative to 0-h sample.

For tobacco alkaloid analysis on clean glass, a targeted MS/MS approach was used. The MS/MS spectra ensured that only the signal from the molecules of interest were being studied because, as discussed previously, the fragmentation

pattern is specific to each given compound. Nicotine signal decreased to about 4% of its initial abundance while nicotine oxide signal increased about 3-fold. The relative increase in nicotine oxide was much lower in this experiment than the initial suspect screening, which is an indicator of experiment-to-experiment variability. Cotinine, N-formylnornicotine, and nicotelline remained relatively constant over the 1-week period. This stability suggests consistent deposition and extraction and that very little partitioning is occurring on clean glass systems.

4.5. TCEP Analysis

TCEP, an antioxidant, was used as an indicator of oxidative potential due to the presence of ROS in THS films. The decay of TCEP and the formation of TCEP oxide was monitored in addition to the temporal trends of the tobacco-related compounds (Figure 8a). Over the course of the week, TCEP decayed to 2% of its initial abundance and TCEP oxide increased to 150% of its initial abundance. The discrepancy indicates that TCEP is also likely being consumed via another reaction. In the absence of THS, TCEP films are stable over the course of one week (i.e. does not oxidize or degrade under ambient air), so changes observed can be attributed to the presence of deposited cigarette smoke (Figure 8b). In the presence of TCEP, the temporal trends of some of the tobacco alkaloids are notably different than on clean glass. Both nicotine oxide diastereomers increased to approximately the same degree as on clean glass, indicating that the

presence of an antioxidant does not completely quench the ROS in deposited cigarette smoke. Nicotelline remained relatively stable over time, indicating that changes in compound abundances can be attributed to legitimate temporal trends of the surface chemicals and not to inconsistencies in deposition or extraction. Nicotine, cotinine, and N-formylnornicotine increased over time, likely due to partitioning. Since this partitioning effect was not present on clean glass, we hypothesize that the addition of a surface film acts as a deep reservoir for SVOCs (a class which includes but is not limited to cotinine, N-formylnornicotine, and nicotine) to partition onto the surface.
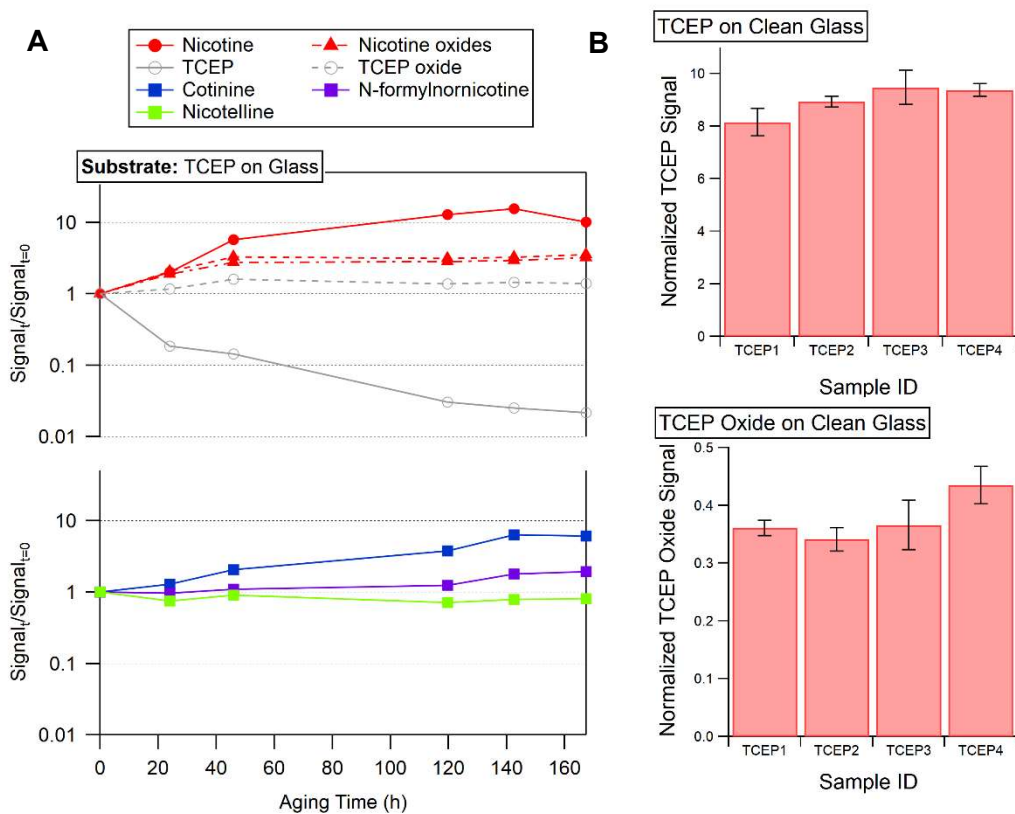
Figure 8. Relative quantitative analysis of tobacco alkaloids on TCEP-coated glass. (A) Relative temporal trends of the tobacco alkaloids. (B) Stability of TCEP on glass in ambient-air-filled jars over time, normalized to the IS signal. The sample IDs TCEP1, TCEP2, TCEP3, and TCEP4 represent time points 19 h, 43 h, 67 h, and 91 h, respectively. The small amounts of TCEP oxide present in these analyses were likely from oxide already present in the solution.

4.6. Surface Film Analysis

To better approximate the effects of THS on indoor environments, common indoor surface film components were deposited onto glass substrates.[12] The chemicals chosen for study included bisphenol A, bis(2-ethylhexyl) sebacate, oleic acid, and squalene (Figure 9). Each contaminant tested contained distinct functional groups that could potentially participate in oxidation reactions with the ROS. By selecting films of interest in this way, broader conclusions could be made about compounds similar to each of the chemicals tested, along with the possibility of learning more about the chemistry of oxidants present in THS films.
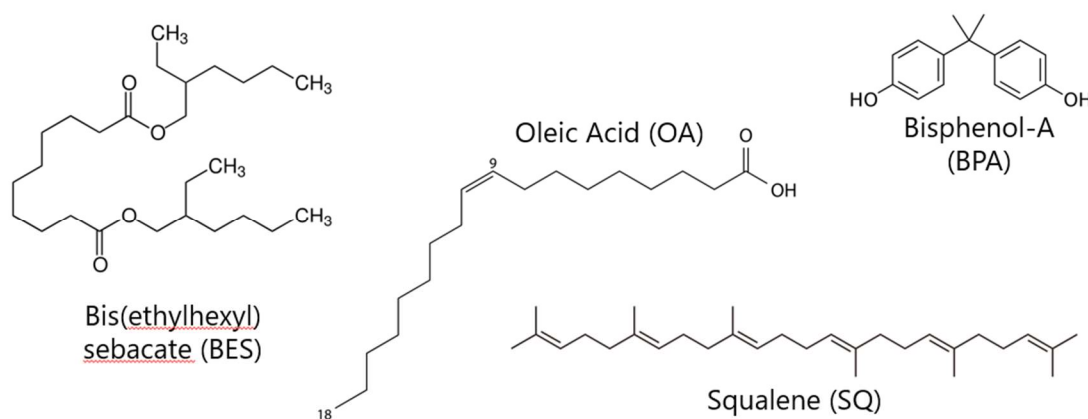
Figure 9. Structures of the surface film chemicals used in this study.

4.6.1. Bisphenol A

Bisphenol A (BPA) is most commonly used in plastic production, so due to the nature of plastic consumption by the general public, there are many routes of exposure on indoor surfaces.[41–43] It has also been shown that oxidation products that are formed by metabolizing BPA can damage and mutate DNA.[44,45] After 1 week, the tobacco alkaloids exhibited similar reactivity and partitioning

Figure 10. Temporal trends of tobacco alkaloids on BPA-coated glass. Change in BPA signal can be attributed to an instrument artifact after 100 h.

as they did in the TCEP studies (Figure 10). Nicotine oxide formation was observed, cotinine and N-formylnornicotine levels increased, and nicotelline levels remained stable. BPA remained relatively constant and products were not observed; however, it is of interest because the BPA film appeared to alter the partitioning behavior of cigarette smoke components when compared to the clean glass trials. The changes observed between the 100-h and 120-h samples were seen in multiple overlapping but unrelated studies, so they can likely be attributed
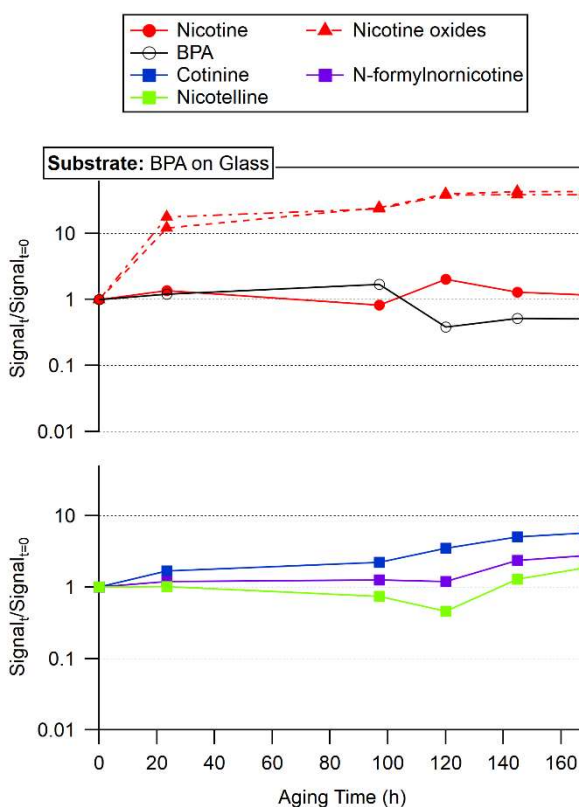
to an instrument artifact. Replicate studies with BPA are needed to better characterize this surface film.

4.6.2. Oleic Acid Product Analysis

At room temperature, oleic acid (OA) is a non-polar, oily liquid, so it did not deposit evenly on the glass substrates. To alleviate this problem, bis(2-ethylhexyl) sebacate (BES) was used as a vehicle to coat the glass with an even layer of OA. BES has been used for this purpose in prior multiphase chemistry studies.[46] Before analyzing the BES+OA films, an experiment was conducted with only BES on glass to investigate how BES films affect THS reactivity and partitioning. The temporal trends revealed that the tobacco alkaloids on BES-coated glass appeared to have behaved similarly to THS on clean glass (Figure 11). Relative to the 0-h sample, very little partitioning occurred over the course of 1 week, which was distinct for film-
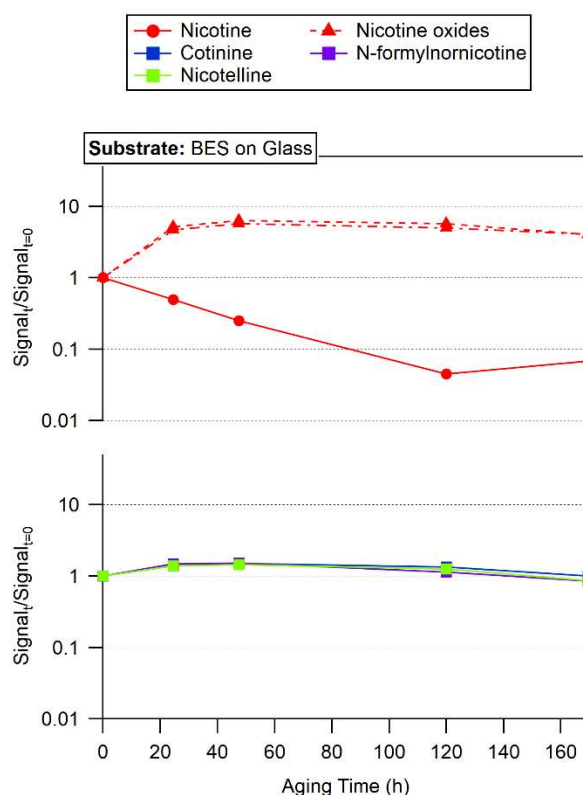
Figure 11. Temporal trends of tobacco alkaloids on BES-coated glass.

coated glass. One possible explanation for this phenomenon is the low viscosity of BES. Surface films are multilayer systems, so the rate of particle partitioning to surface films depends on how fast the molecules can diffuse away from the interface between the condensed and gas phases. A low-viscosity surface film would allow the semi-volatile molecules to diffuse faster into the film, so partitioning of the tobacco alkaloids can occur faster. Based on the temporal trends of cotinine and N-formylnornicotine, it is plausible that most of the partitioning in the system had already occurred by the time the 0-h sample was measured. Further experimentation or kinetic simulations would be required to confirm that partitioning is happening at such an accelerated rate.

Temporal analysis of experiments with OA+BES films indicated that OA is consumed when exposed to THS over the course of a week, so further analysis was needed to identify the products formed. Unreacted OA was observed with a RT of 2.35 min and the deprotonated molecular ion at m/z 281.2493 [M-H]$^{-}$. Two mass-to-charge ratios, labelled mz295 and mz297, with 2 and 3 separated peaks, respectively, were identified as potential OA oxidation products based on their abundances and predicted molecular formulas (Table 7). The extracted ion chromatograms (EICs) for these mass-to-charge ratios indicate that none of these compounds are being co-eluted, so they are likely all different oxidation products (Figure 12). Additionally, none of the compounds eluted at the same time as OA, meaning that they were not the result of oxidation within the ion source of the mass spectrometer.
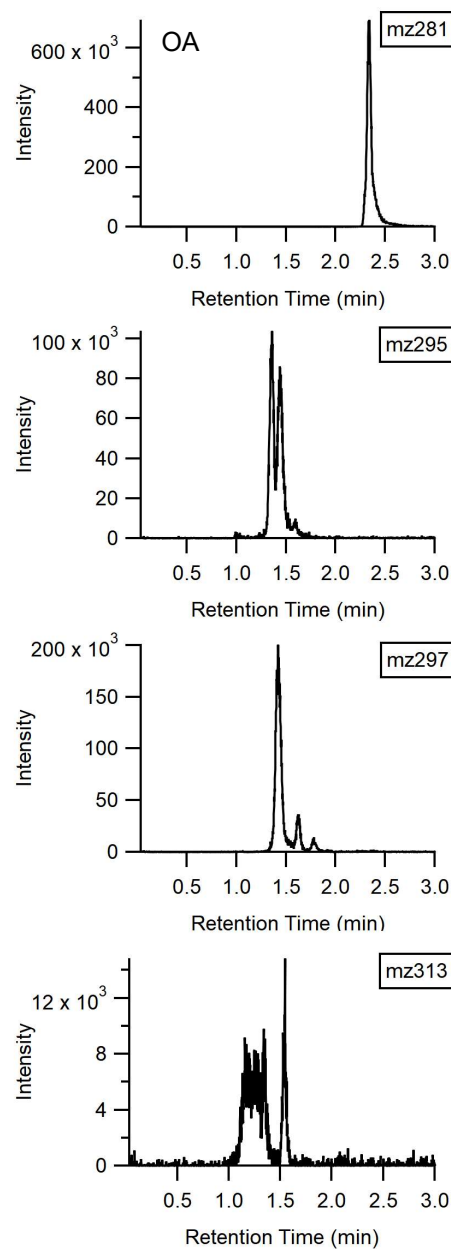
Figure 12. Extracted ion chromatograms of OA and its oxidation products. EICs are extracted with a range of ±0.15 m/z relative to the exact mass.

Fatty acids are known to decompose during the ionization process with a neutral loss of water,[47] supporting the plausibility of detecting [$C_{18}H_{34}O_4$-H_2O-H]$^-$ with m/z 295.2280. In an attempt to support this identification, the data was searched for m/z 313 which would represent $C_{18}H_{34}O_4$ without the neutral loss of water. Upon finding a mass-to-charge ratio with a low m/z difference (2.9 ppm), the ion chromatogram for the intact molecular ion at m/z 313.2388 was extracted and compared to the one for m/z 295.2280. With notably different chromatograms, it does not appear as though mz295 and mz313 co-eluted, so further analysis is needed to attempt to identify the OA oxidation products mz295a and mz295b.

Table 7. M/z values and associated information for OA and its products.

Measured m/z [M-H]$^-$	RT (min)	Label	Predicted Formula	Predicted m/z [M-H]$^-$	m/z diff (ppm)
281.2493	2.35	mz281	[$C_{18}H_{34}O_2$-H]$^-$	281.2481	4.3
295.2280	1.35	mz295a	[$C_{18}H_{34}O_4$-H_2O-H]$^-$	295.2273	2.4
	1.44	mz295b			
297.2438	1.41	mz297a	[$C_{18}H_{34}O_3$-H]$^-$	297.2430	2.7
	1.61	mz297b			
	1.78	mz297b			
313.2388	1.53	mz313	[$C_{18}H_{34}O_4$-H]$^-$	313.2379	2.9

Fatty acids, such as oleic acid, are notoriously hard to fragment using MS/MS. Therefore, to further validate the molecular formula predictions for the isolated compounds, the mass spectral isotope patterns were analyzed. HR-MS is capable of detecting ions with exact masses to a high degree of accuracy, so the natural isotope abundances for elements can be used to help identify molecular formulas of these ions.[48] In many cases, a compound analyzed with mass spectrometry will show a molecular ion peak, which represents the intact (ionized) molecule with the highest natural isotope abundances (e.g., carbon-12, oxygen-16). However, 1.1% of all naturally occurring carbon atoms will be carbon-13, so a smaller mass spectral peak proportional to the number of carbon atoms in the compound will exist one mass unit above the molecular ion peak. Analogous peaks at even higher masses may exist depending on the number of atoms in the compound of interest and the isotope patterns of the elements that comprise the compound. Therefore, natural isotope patterns can be used as supporting information for the molecular formulas of the OA products. Molecular formula generation was performed with Agilent MassHunter Qualitative Analysis 10.0, which uses both exact mass and isotope ratio fitting to annotate mass spectra with formulas.

Based on the isotope pattern analyses, the molecular formula predictions were further supported, allowing for speculations about the chemical structure to be made. Hydroxyl radicals are well-known to participate in reactions with unsaturated hydrocarbons, with one mechanism being peroxidation.[49] A

peroxidation reaction would result in the addition of two oxygens, which is consistent with the molecular formula prediction for mz295 before water is lost during ionization. Due to the nature of the alkene, a hydroperoxide could be added to either side of the double bond, which may explain the two different isomers detected with m/z 295.2280. Further analysis would be needed to support these putative assignments. A planned future experiment would involve reacting OA with hydrogen peroxide to produce hydroperoxide products and analyzing the resulting chromatograms and mass spectra. Similarities between the hydroperoxide products and the isomers observed in this study would indicate that hydroperoxides likely form as a result of THS exposure. Another well-known oxidation mechanism for unsaturated lipids is epoxidation,[50,51] which results in the addition of a single oxygen, consistent with the molecular formula prediction for mz297. The presence of 3 isomers with m/z 297.2438 indicates that there may be different products forming in addition to the epoxide, since there is only one alkene in OA. Further analysis is needed to investigate the structures of these isomers.

4.6.3. Squalene Product Analysis

When exposed to THS, SQ degraded over the course of 1 week. Qualitative analysis revealed a clear signal for remaining SQ (m/z 411.3986) and two mass-to-charge ratios that were potential oxidation products: m/z 425.3779 and m/z 427.3935 (Table 8). In both of the oxidation products' EICs, there is a peak at 13.61 min that represents the in-source ionization of squalene due to peak co-elution with the EIC of m/z 411.3986 (Figure 13). In addition to the co-elution peak, mz425 has 3 prominent chromatographic peaks along with smaller discernible features and mz427 has 1 chromatographic peak. Since mz425 and mz427 do not co-elute, they are likely different compounds, so further experiments were carried out to support molecular formula predictions.
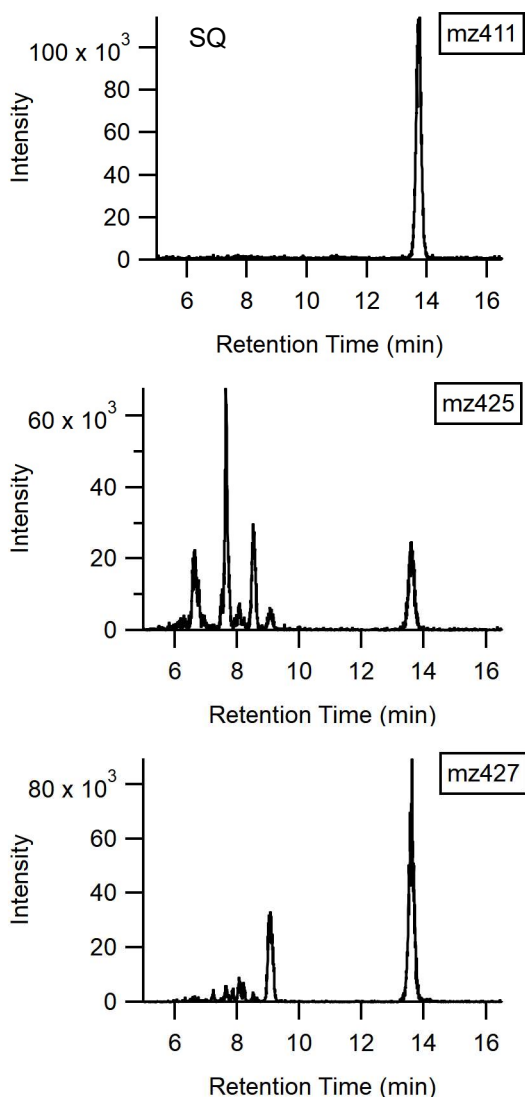

Figure 13. Extracted ion chromatograms of SQ and its oxidation products. EICs are extracted with a range of ±0.15 m/z relative to the exact mass.

Table 8. M/z values and associated information for SQ and its products.

Measured m/z [M+H]$^+$	RT (min)	Label	Predicted Formula	Predicted m/z [M+H]$^+$	m/z diff (ppm)
411.3986	13.61	mz411	[C$_{30}$H$_{50}$+H]$^+$	411.3991	1.2
425.3779	6.63	mz425a	[C$_{30}$H$_{50}$O$_2$-H$_2$O+H]$^+$	425.3783	0.9
	7.65	mz425b			
	8.52	mz425c			
427.3935	9.05	mz427	[C$_{30}$H$_{50}$O+H]$^+$	427.3940	1.2

MS/MS spectra for the predicted SQ oxidation products were used to confirm that the isomers had different chemical structures and led to structural predictions upon further analysis. MS/MS spectra for mz425 and mz427 are displayed in Figure 14 and Figure 15, respectively. The MS/MS spectra for the three isomers for mz425 are all notably different, which indicates that they are all different constitutional isomers. Each oxidation product has a fragment that corresponds to [M-18], i.e. the loss of water. This indicates that these products may share a common functional group. Addition of two oxygen atoms and loss of water would result in m/z 425.3779 and addition of one oxygen atom would result in m/z 427.3935. This is a similar pattern as seen with the OA products, which indicates that similar structures could be expected.

It is fairly reasonable to speculate that m/z 427 results from the formation of an epoxide because there are only so many ways that a single oxygen atom can

be added to an alkene while conserving the number of hydrogens. However, unlike OA, SQ has 6 alkenes instead of 1. Therefore, there are many more ways that two oxygen atoms can be added to SQ, so the identity of m/z 425 is less certain. It is well-documented that squalene hydroperoxides (SQOOHs) can form under oxidative stress.[52] Some studies have shown that these SQOOHs can cause adverse skin effects in humans.[2–5] These hydroperoxides can form at any of the unsaturated carbons present on squalene, so it is possible that at least one of the isomers detected in this study was a SQOOH isomer. However, other studies have indicated the formation of other oxidation products. For example, Eudier et al. proposed a structure that contains an epoxide and an alcohol for a compound with an nominal mass-to-charge ratio of 425.[53] If the compound in this study had a similar chemical structure, then the presence of an epoxide would explain the similar fragmentation pattern to m/z 427. Further experimentation and analysis, such as reacting SQ with hydrogen peroxide or other readily available ROS to identify similarities, would be needed to formulate better predictions for the separated isomers.
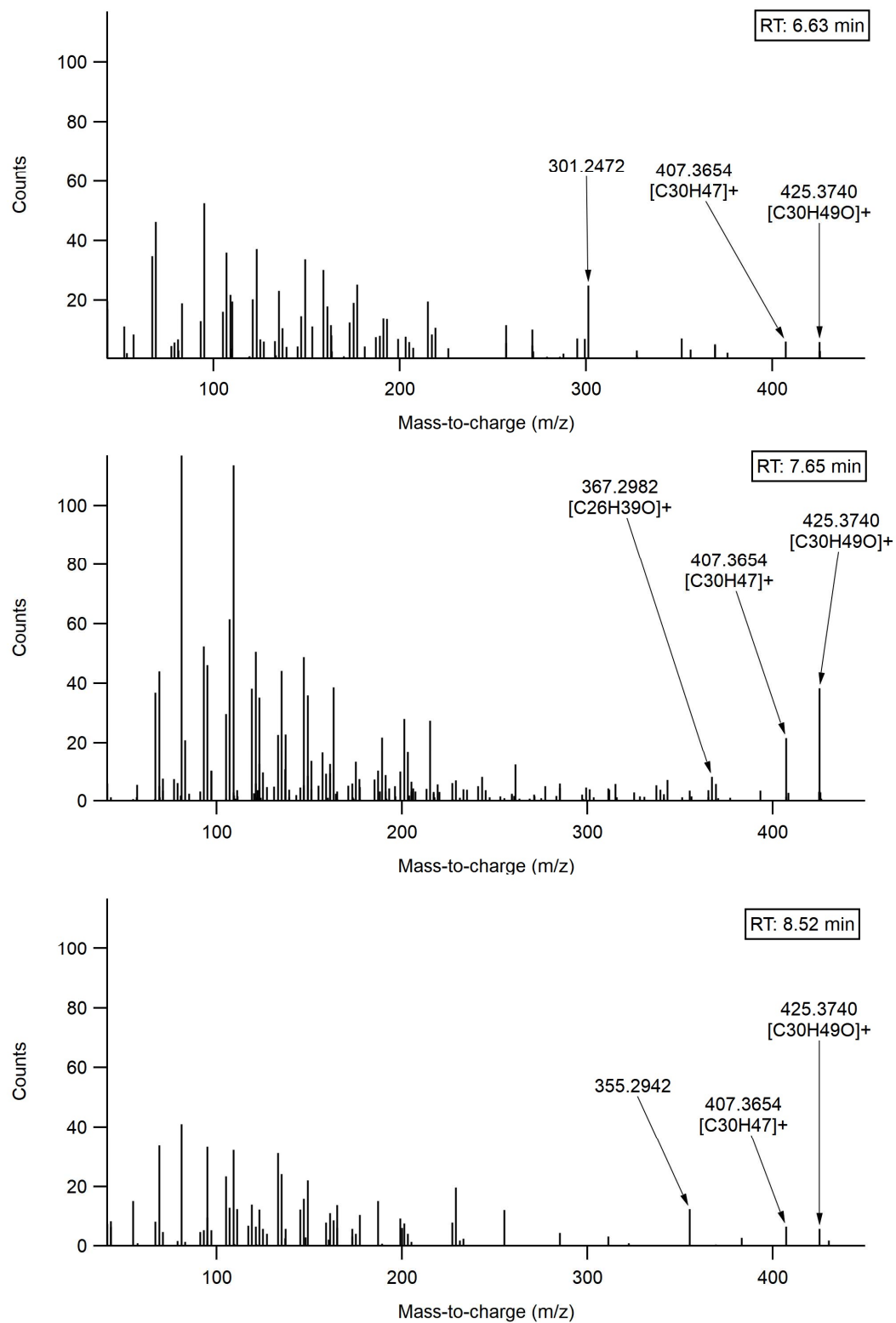
Figure 14. MS/MS spectra for m/z 425.3740 isomers. Fragments characteristic to each isomer are labeled with their mass-to-charge ratios and molecular formula matches.
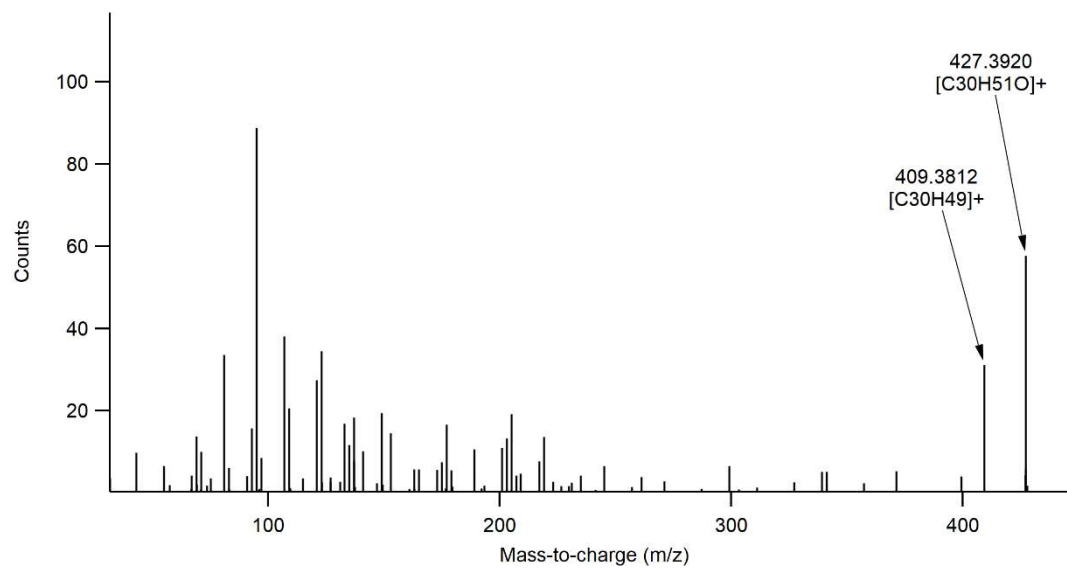
Figure 15. MS/MS spectra for m/z 427.3920. Fragments characteristic to the compound are labeled with their mass-to-charge ratios and molecular formula matches.

4.7. Preliminary Fabric Analysis: Cellulose Model

To better approximate the wide variety of materials found in indoor environments, non-glass substrates need to be considered. Preliminary studies investigated cellulose filter paper, an organic polymer arranged into a microscopically porous paper material, which can be used as a model system for common indoor surfaces such as wood or paper-based materials. The temporal trends of tobacco alkaloids were investigated to see how they compared to the clean glass experiments. Both oxidation and partitioning were observed: the nicotine oxide diastereomers formed and the amount of cotinine and N-formylnornicotine on the surface increased over the course of 1 week (Figure 16). These trends indicated that a porous surface causes the THS compounds to behave similar to when a surface film is deposited; the porous surface acts as a sink for partitioning to occur, perhaps due to the far higher surface area than the flat glass surface.

Figure 16. Temporal trends of tobacco alkaloids on clean cellulose.

5. Conclusion

In this thesis, I discussed the complex relationship between deposited cigarette smoke residue and the surface on which it is deposited. The results indicated that not only does THS act as a source of ROS to oxidize the surface films through multiple different oxidation mechanisms but also that the presence of a surface film has the capacity to change the temporal trends of the deposited tobacco alkaloids. Depositing THS onto OA- and SQ-coated substrates resulted in the formation of multiple oxidation products. While the identification of chemical structures for many of the products observed in these experiments is still underway, HR-MS allowed for confident predictions about the molecular formulas for these products.

The experiments discussed in this thesis have delved into the oxidation of alkene-rich surface films (OA and SQ) on clean glass when exposed to THS. However, due to the diversity of indoor pollutants, surface materials, and sources of ROS in indoor environments, more work is needed to better characterize the surface chemistry of deposited particles. Expanding the variety of surface films studied to include models for flame retardants, pesticides, cleaning products, and other common household contaminants would allow for a more generalizable conclusion about the reactivity of indoor surface films. Additionally, by studying the oxidation processes on other substrates such as cellulose, nylon, and polyester, the effects of specific materials on the reactivity and composition of the surface

films can be probed. Finally, exploring the oxidation of surface films caused by wood smoke and cooking emissions can highlight differences in ROS sources that can interact with indoor surfaces. The consideration of these three factors would allow for a more holistic picture of indoor surface chemistry to be realized.

References

(1) Klepeis, N. E.; Nelson, W. C.; Ott, W. R.; Robinson, J. P.; Tsang, A. M.; Switzer, P.; Behar, J. V.; Hern, S. C.; Engelmann, W. H. The National Human Activity Pattern Survey (NHAPS): A Resource for Assessing Exposure to Environmental Pollutants. *J Expo Sci Environ Epidemiol* **2001**, *11* (3), 231–252. https://doi.org/10.1038/sj.jea.7500165.

(2) Chiba, K.; Kawakami, K.; Sone, T.; Onoue, M. Characteristics of Skin Wrinkling and Dermal Changes Induced by Repeated Application of Squalene Monohydroperoxide to Hairless Mouse Skin. *SPP* **2003**, *16* (4), 242–251. https://doi.org/10.1159/000070847.

(3) Chiba, K.; Yoshizawa, K.; Makino, I.; Kawakami, K.; Onoue, M. Comedogenicity of Squalene Monohydroperoxide in the Skin After Topical Application. *The Journal of Toxicological Sciences* **2000**, *25* (2), 77–83. https://doi.org/10.2131/jts.25.77.

(4) Ottaviani, M.; Alestas, T.; Flori, E.; Mastrofrancesco, A.; Zouboulis, C. C.; Picardo, M. Peroxidated Squalene Induces the Production of Inflammatory Mediators in HaCaT Keratinocytes: A Possible Role in Acne Vulgaris. *Journal of Investigative Dermatology* **2006**, *126* (11), 2430–2437. https://doi.org/10.1038/sj.jid.5700434.

(5) Ryu, A.; Arakane, K.; Koide, C.; Arai, H.; Nagano, T. Squalene as a Target Molecule in Skin Hyperpigmentation Caused by Singlet Oxygen. *Biological and Pharmaceutical Bulletin* **2009**, *32* (9), 1504–1509. https://doi.org/10.1248/bpb.32.1504.

(6) Breen, M.; Burke, J.; Batterman, S.; Vette, A.; Godwin, C.; Croghan, C.; Schultz, B.; Long, T. Modeling Spatial and Temporal Variability of Residential Air Exchange Rates for the Near-Road Exposures and Effects of Urban Air Pollutants Study (NEXUS). *IJERPH* **2014**, *11* (11), 11481–11504. https://doi.org/10.3390/ijerph111111481.

(7) Brown, S. K.; Sim, M. R.; Abramson, M. J.; Gray, C. N. Concentrations of Volatile Organic Compounds in Indoor Air - A Review. *Indoor Air* **1994**, *4* (2), 123–134. https://doi.org/10.1111/j.1600-0668.1994.t01-2-00007.x.

(8) Abbatt, J. P. D.; Wang, C. The Atmospheric Chemistry of Indoor Environments. *Environ. Sci.: Processes Impacts* **2020**, *22* (1), 25–48. https://doi.org/10.1039/C9EM00386J.

(9) Ault, A. P.; Grassian, V. H.; Carslaw, N.; Collins, D. B.; Destaillats, H.; Donaldson, D. J.; Farmer, D. K.; Jimenez, J. L.; McNeill, V. F.; Morrison, G. C.; O'Brien, R. E.; Shiraiwa, M.; Vance, M. E.; Wells, J. R.; Xiong, W. Indoor Surface Chemistry: Developing a Molecular Picture of Reactions on Indoor Interfaces. *Chem* **2020**, *6* (12), 3203–3218. https://doi.org/10.1016/j.chempr.2020.08.023.

(10) Weschler, C. J.; Carslaw, N. Indoor Chemistry. *Environ. Sci. Technol.* **2018**, *52* (5), 2419–2428. https://doi.org/10.1021/acs.est.7b06387.

(11) Grant, J. S.; Zhu, Z.; Anderton, C. R.; Shaw, S. K. Physical and Chemical Morphology of Passively Sampled Environmental Films. *ACS Earth Space Chem.* **2019**, *3* (2), 305–313. https://doi.org/10.1021/acsearthspacechem.8b00158.

(12) Weschler, C. J.; Nazaroff, W. W. Growth of Organic Films on Indoor Surfaces. *Indoor Air* **2017**, *27* (6), 1101–1112. https://doi.org/10.1111/ina.12396.

(13) Wang, C.; Collins, D. B.; Arata, C.; Goldstein, A. H.; Mattila, J. M.; Farmer, D. K.; Ampollini, L.; DeCarlo, P. F.; Novoselac, A.; Vance, M. E.; Nazaroff, W. W.; Abbatt, J. P. D. Surface Reservoirs Dominate Dynamic Gas-Surface Partitioning of Many Indoor Air Constituents. *Sci. Adv.* **2020**, *6* (8), eaay8973. https://doi.org/10.1126/sciadv.aay8973.

(14) Skoog, D. A.; Holler, F. J.; Crouch, S. R. *Principles of Instrumental Analysis*, Seventh edition.; Cengage Learning: Australia, 2018.

(15) Xian, F.; Hendrickson, C. L.; Marshall, A. G. High Resolution Mass Spectrometry. *Anal. Chem.* **2012**, *84* (2), 708–719. https://doi.org/10.1021/ac203191t.

(16) McLafferty, F. W. Tandem Mass Spectrometry. *Science* **1981**, *214* (4518), 280–287. https://doi.org/10.1126/science.7280693.

(17) Weschler, C. J.; Nazaroff, W. W. Semivolatile Organic Compounds in Indoor Environments. *Atmospheric Environment* **2008**, *42* (40), 9018–9040. https://doi.org/10.1016/j.atmosenv.2008.09.052.

(18) Pryor, W. A.; Stone, K. Oxidants in Cigarette Smoke Radicals, Hydrogen Peroxide, Peroxynitrate, and Peroxynitritea. *Annals of the New York Academy of Sciences* **1993**, *686* (1), 12–27. https://doi.org/10.1111/j.1749-6632.1993.tb39148.x.

(19) Acuff, L.; Fristoe, K.; Hamblen, J.; Smith, M.; Chen, J. Third-Hand Smoke: Old Smoke, New Concerns. *J Community Health* **2016**, *41* (3), 680–687. https://doi.org/10.1007/s10900-015-0114-1.

(20) DeCarlo, P. F.; Avery, A. M.; Waring, M. S. Thirdhand Smoke Uptake to Aerosol Particles in the Indoor Environment. *Science Advances* **2018**, *4* (5), eaap8368. https://doi.org/10.1126/sciadv.aap8368.

(21) Ramírez, N.; Özel, M. Z.; Lewis, A. C.; Marcé, R. M.; Borrull, F.; Hamilton, J. F. Exposure to Nitrosamines in Thirdhand Tobacco Smoke Increases Cancer Risk in Non-Smokers. *Environ. Int.* **2014**, *71*, 139–147. https://doi.org/10.1016/j.envint.2014.06.012.

(22) Sleiman, M.; Gundel, L. A.; Pankow, J. F.; Jacob, P.; Singer, B. C.; Destaillats, H. Formation of Carcinogens Indoors by Surface-Mediated Reactions of Nicotine with Nitrous Acid, Leading to Potential Thirdhand Smoke Hazards. *Proceedings of the National Academy of Sciences* **2010**, *107* (15), 6576–6581. https://doi.org/10.1073/pnas.0912820107.

(23) Matt, G. E.; Quintana, P. J. E.; Hovell, M. F.; Bernert, J. T.; Song, S.; Novianti, N.; Juarez, T.; Floro, J.; Gehrman, C.; Garcia, M.; Larson, S. Households Contaminated by Environmental Tobacco Smoke: Sources of Infant Exposures. *Tob Control* **2004**, *13* (1), 29. https://doi.org/10.1136/tc.2003.003889.

(24) Martins-Green, M.; Adhami, N.; Frankos, M.; Valdez, M.; Goodwin, B.; Lyubovitsky, J.; Dhall, S.; Garcia, M.; Egiebor, I.; Martinez, B.; Green, H. W.; Havel, C.; Yu, L.; Liles, S.; Matt, G.; Destaillats, H.; Sleiman, M.; Gundel, L. A.; Benowitz, N.; Jacob, P.; Hovell, M.; Winickoff, J. P.; Curras-Collazo, M. Cigarette Smoke Toxins Deposited on Surfaces: Implications for Human Health. *PLoS One* **2014**, *9* (1), e86391. https://doi.org/10.1371/journal.pone.0086391.

(25) Hang, B.; Wang, P.; Zhao, Y.; Chang, H.; Mao, J.-H.; Snijders, A. M. Thirdhand Smoke: Genotoxicity and Carcinogenic Potential. *Chronic Dis Transl Med.* **2019**. https://doi.org/10.1016/j.cdtm.2019.08.002.

(26) Sleiman, M.; Destaillats, H.; Smith, J. D.; Liu, C.-L.; Ahmed, M.; Wilson, K. R.; Gundel, L. A. Secondary Organic Aerosol Formation from Ozone-Initiated Reactions with Nicotine and Secondhand Tobacco Smoke. *Atmos. Environ.* **2010**, *44* (34), 4191–4198. https://doi.org/10.1016/j.atmosenv.2010.07.023.

(27) Petrick, L. M.; Sleiman, M.; Dubowski, Y.; Gundel, L. A.; Destaillats, H. Tobacco Smoke Aging in the Presence of Ozone: A Room-Sized Chamber Study. *Atmospheric Environment* **2011**, *45* (28), 4959–4965. https://doi.org/10.1016/j.atmosenv.2011.05.076.

(28) Sleiman, M.; Logue, J. M.; Luo, W.; Pankow, J. F.; Gundel, L. A.; Destaillats, H. Inhalable Constituents of Thirdhand Tobacco Smoke: Chemical Characterization and Health Impact Considerations. *Environ. Sci. Technol.* **2014**, *48* (22), 13093–13101. https://doi.org/10.1021/es5036333.

(29) Destaillats, H.; Singer, B. C.; Lee, S. K.; Gundel, L. A. Effect of Ozone on Nicotine Desorption from Model Surfaces: Evidence for Heterogeneous Chemistry. *Environ. Sci. Technol.* **2006**, *40* (6), 1799–1805. https://doi.org/10.1021/es050914r.

(30) Tuet, W. Y.; Liu, F.; de Oliveira Alves, N.; Fok, S.; Artaxo, P.; Vasconcellos, P.; Champion, J. A.; Ng, N. L. Chemical Oxidative Potential and Cellular Oxidative Stress from Open Biomass Burning Aerosol. *Environ. Sci. Technol. Lett.* **2019**, *6* (3), 126–132. https://doi.org/10.1021/acs.estlett.9b00060.

(31) Daellenbach, K. R.; Uzu, G.; Jiang, J.; Cassagnes, L.-E.; Leni, Z.; Vlachou, A.; Stefenelli, G.; Canonaco, F.; Weber, S.; Segers, A.; Kuenen, J. J. P.; Schaap, M.; Favez, O.; Albinet, A.; Aksoyoglu, S.; Dommen, J.; Baltensperger, U.; Geiser, M.; El Haddad, I.; Jaffrezo, J.-L.;

Prévôt, A. S. H. Sources of Particulate-Matter Air Pollution and Its Oxidative Potential in Europe. *Nature* **2020**, *587* (7834), 414–419. https://doi.org/10.1038/s41586-020-2902-8.

(32) Hammond, D.; Wiebel, F.; Kozlowski, L. T.; Borland, R.; Cummings, K. M.; O'Connor, R. J.; McNeill, A.; Connolly, G. N.; Arnott, D.; Fong, G. T. Revising the Machine Smoking Regime for Cigarette Emissions: Implications for Tobacco Control Policy. *Tob Control* **2007**, *16* (1), 8–14. https://doi.org/10.1136/tc.2005.015297.

(33) *Chemistry and Toxicology of Cigarette Smoke and Biomarkers of Exposure and Harm*; Centers for Disease Control and Prevention (US), 2010.

(34) Benowitz, N. L.; Hukkanen, J.; Jacob, P. Nicotine Chemistry, Metabolism, Kinetics and Biomarkers. In *Nicotine Psychopharmacology*; Henningfield, J. E., London, E. D., Pogun, S., Eds.; Hofmann, F. B., Series Ed.; Handbook of Experimental Pharmacology; Springer Berlin Heidelberg: Berlin, Heidelberg, 2009; Vol. 192, pp 29–60. https://doi.org/10.1007/978-3-540-69248-5_2.

(35) Benowitz, N. L. Biomarkers of Environmental Tobacco Smoke Exposure. *Environ. Health Perspect.* **1999**, *107* (suppl 2), 349–355. https://doi.org/10.1289/ehp.99107s2349.

(36) Whitehead, T. P.; Havel, C.; Metayer, C.; Benowitz, N. L.; Jacob, P. Tobacco Alkaloids and Tobacco-Specific Nitrosamines in Dust from Homes of Smokeless Tobacco Users, Active Smokers, and Nontobacco Users. *Chem. Res. Toxicol.* **2015**, *28* (5), 1007–1014. https://doi.org/10.1021/acs.chemrestox.5b00040.

(37) Jacob, P.; Goniewicz, M. L.; Havel, C. M.; Schick, S. F.; Benowitz, N. L. Nicotelline: A Proposed Biomarker and Environmental Tracer for Particulate Matter Derived from Tobacco Smoke. *Chem. Res. Toxicol.* **2013**, *26* (11), 1615–1631. https://doi.org/10.1021/tx400094y.

(38) Jin, M.; Earla, R.; Shah, A.; Earla, R. L.; Gupte, R.; Mitra, A. K.; Kumar, A.; Kumar, S. A LC-MS/MS Method for Concurrent Determination of Nicotine Metabolites and Role of CYP2A6 in Nicotine Metabolism in U937 Macrophages: Implications in Oxidative Stress in HIV + Smokers. *J Neuroimmune Pharmacol* **2012**, *7* (1), 289–299. https://doi.org/10.1007/s11481-011-9283-6.

(39) Zhang, X.; Wang, R.; Zhang, L.; Ruan, Y.; Wang, W.; Ji, H.; Lin, F.; Liu, J. Simultaneous Determination of Tobacco Minor Alkaloids and Tobacco-Specific Nitrosamines in Mainstream Smoke by Dispersive Solid-Phase Extraction Coupled with Ultra-Performance Liquid Chromatography/Tandem Orbitrap Mass Spectrometry. *Rapid Commun Mass Spectrom* **2018**, *32* (20), 1791–1798. https://doi.org/10.1002/rcm.8222.

(40) Smyth, T. J.; Ramachandran, V. N.; McGuigan, A.; Hopps, J.; Smyth, W. F. Characterisation of Nicotine and Related Compounds Using Electrospray Ionisation with Ion Trap Mass Spectrometry and with Quadrupole Time-of-Flight Mass Spectrometry and Their Detection by Liquid Chromatography/Electrospray Ionisation Mass Spectrometry. *Rapid Communications in Mass Spectrometry* **2007**, *21* (4), 557–566. https://doi.org/10.1002/rcm.2871.

(41) Staples, C. A.; Dome, P. B.; Klecka, G. M.; Oblock, S. T.; Harris, L. R. A Review of the Environmental Fate, Effects, and Exposures of Bisphenol A. *Chemosphere* **1998**, *36* (10), 2149–2173. https://doi.org/10.1016/S0045-6535(97)10133-3.

(42) Caban, M.; Stepnowski, P. Determination of Bisphenol A in Size Fractions of Indoor Dust from Several Microenvironments. *Microchemical Journal* **2020**, *153*, 104392. https://doi.org/10.1016/j.microc.2019.104392.

(43) Deborde, M.; Rabouan, S.; Mazellier, P.; Duguet, J.-P.; Legube, B. Oxidation of Bisphenol A by Ozone in Aqueous Solution. *Water Research* **2008**, *42* (16), 4299–4308. https://doi.org/10.1016/j.watres.2008.07.015.

(44) Atkinson, A.; Roy, D. In Vivo DNA Adduct Formation by Bisphenol A. *Environ. Mol. Mutagen.* **1995**, *26* (1), 60–66. https://doi.org/10.1002/em.2850260109.

(45) Kolšek, K.; Mavri, J.; Sollner Dolenc, M. Reactivity of Bisphenol A-3,4-Quinone with DNA. A Quantum Chemical Study. *Toxicology in Vitro* **2012**, *26* (1), 102–106. https://doi.org/10.1016/j.tiv.2011.11.003.

(46) Zhou, S.; Hwang, B. C. H.; Lakey, P. S. J.; Zuend, A.; Abbatt, J. P. D.; Shiraiwa, M. Multiphase Reactivity of Polycyclic Aromatic Hydrocarbons Is Driven by Phase Separation

and Diffusion Limitations. *PNAS* **2019**, *116* (24), 11658–11663. https://doi.org/10.1073/pnas.1902517116.

(47) Murphy, R. C.; Axelsen, P. H. Mass Spectrometric Analysis of Long-Chain Lipids. *Mass Spectrom Rev* **2011**, *30* (4), 579–599. https://doi.org/10.1002/mas.20284.

(48) McLafferty, F. W.; Tureček, F. *Interpretation of Mass Spectra*, 4th ed.; University Science Books: Mill Valley, Calif, 1993.

(49) Ayala, A.; Muñoz, M. F.; Argüelles, S. Lipid Peroxidation: Production, Metabolism, and Signaling Mechanisms of Malondialdehyde and 4-Hydroxy-2-Nonenal. *Oxid Med Cell Longev* **2014**, *2014*, 360438. https://doi.org/10.1155/2014/360438.

(50) Schaich, K. M.; Xie, J.; Bogusz, B. A. Thinking Outside the Classical Chain Reaction Box of Lipid Oxidation: Evidence for Alternate Pathways and the Importance of Epoxides. *Lipid Technology* **2017**, *29* (9–10), 91–96. https://doi.org/10.1002/lite.201700025.

(51) Boerkamp, V. J. P.; Merkx, D. W. H.; Wang, J.; Vincken, J.-P.; Hennebelle, M.; van Duynhoven, J. P. M. Quantitative Assessment of Epoxide Formation in Oil and Mayonnaise by 1H-13C HSQC NMR Spectroscopy. *Food Chemistry* **2022**, *390*, 133145. https://doi.org/10.1016/j.foodchem.2022.133145.

(52) Shimizu, N.; Ito, J.; Kato, S.; Eitsuka, T.; Saito, T.; Nishida, H.; Miyazawa, T.; Nakagawa, K. Evaluation of Squalene Oxidation Mechanisms in Human Skin Surface Lipids and Shark Liver Oil Supplements. *Ann. N.Y. Acad. Sci.* **2019**, *1457* (1), 158–165. https://doi.org/10.1111/nyas.14219.

(53) Eudier, F.; Hucher, N.; Picard, C.; Savary, G.; Grisel, M. Squalene Oxidation Induced by Urban Pollutants: Impact on Skin Surface Physico-Chemistry. *Chem. Res. Toxicol.* **2019**, *32* (2), 285–293. https://doi.org/10.1021/acs.chemrestox.8b00311.